AI-CHD: An AI-based Framework for Cost-Effective Surgical Telementoring of Congenital Heart Disease

Xiaowe Xu[1*], Haiyun Yuan[2*], Hailong Qiu[2*], Yiyu Shi[3], Qianjun Jia[4], Zeyang Yao[2], Wen Xie[2], Huiming Guo[1], Meiping Huang[4†], Jian Zhuang[2†]

[1] *Guangdong Provincial Key Laboratory of South China Structural Heart Disease, Guangdong Provincial People's Hospital, Guangdong Academy of Medical Sciences, Guangzhou, China, 510080*

[2] *Guangdong Cardiovascular Institute, Guangdong Provincial Key Laboratory of South China Structural Heart Disease, Guangdong Provincial People's Hospital, Guangdong Academy of Medical Sciences, Guangzhou, China, 510080*

[3]*Department of Computer Science and Engneering, University of Notre Dame, IN, US, 46556*

[4]*Department of Catheterization Lab, Guangdong Cardiovascular Institute, Guangdong Provincial Key Laboratory of South China Structural Heart Disease, Guangdong Provincial People's Hospital, Guangdong Academy of Medical Sciences, Guangzhou, China, 510080*

1 Introduction

Congenital heart disease (CHD) is the most common congenital birth defect, which has long been known as one of the main causes of death in the first year of life. Every year there are more than one million babies born with CHD out of the approximately 130 million newborns in the world. Cardiac surgery has been a major way to effectively tackle CHD, and over the last century, its remarkable advances has led to decreased mortality rate of newborns with CHD.

However, the decreased mortality rate is mostly observed in developed countries rather than developing ones. The main reason is that the surgical treatment of CHD requires complex infrastructures, equipment, and highly skilled surgeons. While developed countries have perfected their treatment of CHD for more than 50 years, developing countries are still at an initial stage. It is estimated that the number of congenital cardiac surgeons need to be increased by 1,250 times to satisfy only basic needs of CHD treatment worldwide [1], and most of those surgeons reside in developed countries. As a result, the mortality rate in developing countries is currently at 20%, which is strikingly higher than that of 3%-7% in developed countries, not to mention the fact that mortality rate in developing countries is likely under-reported due to the lack of proper diagnosis.

2 Remote Surgery

Remote surgery has been an active field for decades which enables experienced surgeons to provide instructions to robots (telerobotics) or guidance to less-experienced surgeons (surgical telementoring) remotely. It can help deliver high-quality surgeon expertise from developed countries to developing countries, or from high-end urban medical centers to rural hospitals within developing countries.

Telerobotics enables surgeons to control robots remotely in a master-slave manner. Stable camera systems are implemented in both sites. On the robot site, multiple cameras are used to construct a virtual image of the operative field which is provided to the surgeon site. On the surgeon site, multiple cameras are adopted to capture the movements of the surgeon's hand using three-dimensional (3-D) imaging systems. Such movements are further sent to the robot site and simulated by the robot operating on the patient. The images and movements are required to be

*Contributed equally

†Corresponding authors

transmitted in real time, and large latency may affect the surgeon's performance, or even lead to the failure of the surgery. Telerobotics can also let surgeons sit comfortably while performing some delicate operations engaging fine movements. However, due to the highly demanding nature and potential risks, telerobotics has very limited clinic applications. Only a few systems including the Da Vinci [2] and the Zeus [3] are approved for clinical use. At present, telerobotic is still in its early phase.

On the other hand, surgical telementoring consists of an expert surgeon guiding a less experienced surgeon remotely. Such guidance is achieved with real-time audio and video transmission. Thus, the two surgeons can communicate in real-time to discuss the procedure, and the expert surgeon can deliver precise guidance based on the real-time video streaming of the surgery process. Surgical telementoring can be performed in rural areas and austere environments for not only difficult surgeries but also surgery education. Similar to telerobotics, surgical telementoring requires real-time data transmission, but now between locations that are far apart. Fortunately, with the recent 4G or even 5G communication technologies, this problem is mitigated to a great extent. Recently, surgical telementoring has been widely adopted and experimented in clinical use due to the improved transmission quality and less potential risk compared with telerobotic. Though also in its early stage, surgical telementoring is relatively more mature than telerobotics with its relatively lower cost and lower technology complexity.

However, surgical telemonitoring for CHD still faces challenges. First, cardiac surgery for the treatment of CHD is rather complex and is generally regarded as the jewel in the crown of surgery. As such, CHD diagnosis and surgical planning is usually time consuming and thus the cost can be very high for the expertise and time to be delivered remotely, which may not be affordable for developing countries or rural areas. For example, it takes even a very experienced radiologist several hours to examine the medical image of a CHD patient for diagnosis, whereas that time is usually in the order of minutes for common heart diseases. Second, the machine quality and operator skill in developing countries or rural areas may be limited, leading to issues such as low imaging quality under non-ideal settings.

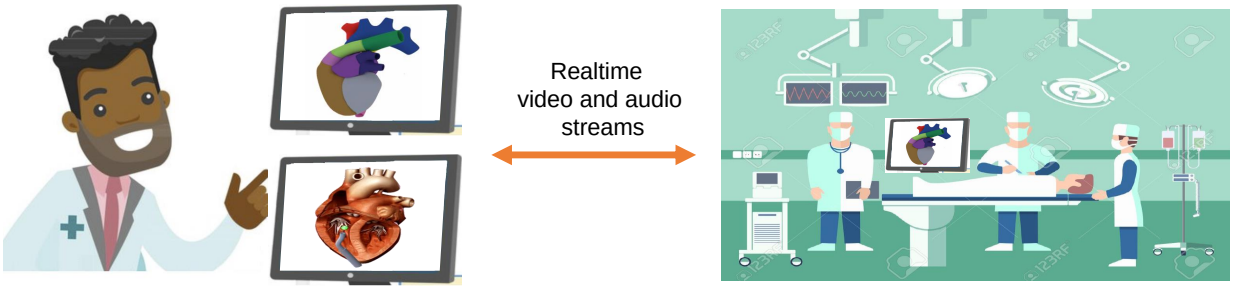

Figure 1: Surgical telementoring: technical assistance and real-time guidance through real-time video and audio streams.

3 AI-CHD

One potential solution to reduce the cost is to involve artificial intelligence (AI) to automatically construct accurate 3D model of heart from medical images, a critical yet otherwise time-consuming process in surgical telementoring of CHD. Before surgery, such a model can be helpful for remote surgical planning and discussion. During surgery, the proper display of the model through augmented reality (AR) or virtual reality (VR) technologies can facilitate communication between the surgeon and the novice, and enhance the operation efficiency.

AI-based framework AI-CHD, our novel solution, aims to provide accurate and efficient heart model construction for surgical telementoring of CHD based on 3D Computed Tomography (CT) images. Considering the fact that the artifact type and pattern in CT images acquired with medium- and low-end machines or limited skills may be different from those in standard training sets, the framework first exploits a weakly supervised way to remove artifacts in a CT image which does not require a prior training set. Further considering the fact that hearts in CHD exhibit large variations in structures and/or great vessel connections without local tissue changes, the framework then deploys hybrid deep learning and graph analysis to tackle the model construction. We performs evaluations of each step with collected datasets and the overall system with a case study.

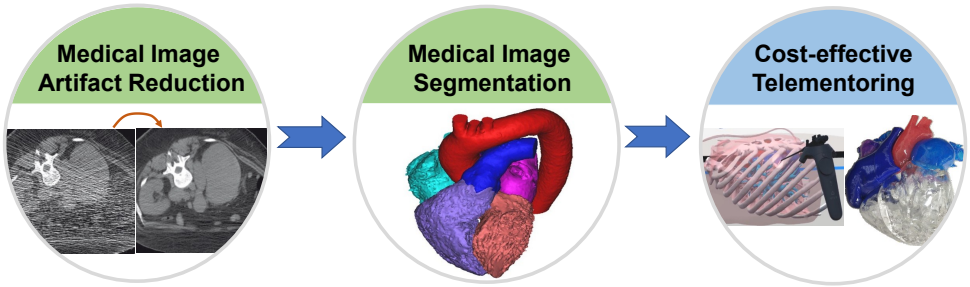

Figure 2: Overall flow of AI-CHD.

3.1 Medical Image Artifact Reduction

Medical images exhibit various types of artifacts with different patterns and their mixtures, which depend on many factors including scan setting, machine condition, patient size and age, surrounding environment, etc. This problem is even worse on medium- and low-end CT imaging machines, operated by less skilled technologists, which are common in rural areas in developing countries. On the other hand, existing deep learning based medical image artifact reduction methods are restricted by the specific training data that contains predetermined artifact types and patterns, which can hardly capture all possibilities exclusively. Accordingly, they can only work well under the scenarios defined by the training data. In this step, we exploit the power of deep learning but without using pre-trained networks for medical artifact reduction. Specifically, at test time we train a light-weight image-specific artifact reduction network using data synthesized from the input image. Without requiring any prior training data, our method can work with almost any medical images that contain varying or unknown artifacts.

The main flow of artifact reduction contains two modules: artifact synthesis and artifact removal. In the first module, radiologists need to annotate a total of 10-20 regions of interest (RoIs) from a 3D input CT image. These RoIs are further used to train a light-weight five-layer synthesis network which synthesizes a large number of paired patches. Note that as different medical images have different ranges of pixel values, we normalize every slice to [0,1] before processing and scale them back afterwards. With synthesized paired patches, theoretically any existing CNN-based artifact reduction networks can be trained. However, a key issue here is that we perform the task on each input image. A deep and complex network may need a large number of paired data and take a long training time. On the other hand, small networks may not attain desired performance. Thus, in the second module, we resort to artifact removal network, a compact attentive generative network architecture that can pay special attention to artifacts and train it adversarially for faster convergence. It is formed by a two-step attentive-recurrent network followed by a 10-layer contextual autoencoder to reduce artifacts and to restore the information obstructed by

them. Once trained, the artifact removal network is finally applied to all slices of the 3D volume for artifact reduction.

Fundamental to our method is the fact that artifacts in most medical images exhibit localized patterns, i.e., they do not cover the entire image uniformly. It is almost always possible to identify within an image "clean" regions (with little artifacts) and "dirty" regions (with significant artifacts). This provides the possibility to synthesize paired dirty-clean training patches from an image with artifacts. In addition, as visual entropy inside a single image is much smaller than in a general external collection of images [4], the synthesized training data does not need to be big and the associated artifact reduction network can be compact and converges fast.

We evaluate the performance of this step with CT images containing different levels of Poisson noise collected by our wide detector 256-slice MDCT scanner with 8 cm of coverage, using the following protocol: collimation, (96-128)$\times$0.625 mm; rotation time, 270 ms, which corresponds to a 135-ms standard temporal resolution; slice thickness, 0.9 mm; reconstruction interval, 0.45 mm. Adaptive axial z-collimation was used to optimize the cranio-caudal length. Data were obtained at 40-50% of the RR interval, utilizing a 5% phase tolerance around the 45% phase. All CT images are qualitatively evaluated by our radiologists on structure preservation and artifact level. For quantitative evaluation, due to the lack of ground truth, we follow most existing works [5, 6] and select the most homogeneous area in regions of interest selected by radiologists. The standard deviation (artifact level) of the pixels in the area should be as low as possible.

Our method trains and tests on each individual patient's image, and no pre-training is involved. We compare our method with the state-of-the-art deep learning based medical image artifact reduction methods CCADN [7], which is trained following exactly the same settings reported. The CT training data set for CCADN contain 100,000 image patches. We consider both the ideal situation where the test images only contain Poisson noise of level similar to that in the training set, and non-ideal situation where the test images have higher level of noises. The results are shown in Figure 3(a). Qualitatively, our method and CCADN preserve structures well for both ideal and non-ideal situations. Ours outperforms CCADN even for the level of noise that CCADN is trained to reduce (the regions in Figure 3(a)(1). Quantitatively, ours beats CCADN in both ideal and non-ideal situations, achieving up to 29.2% lower standard deviation and 18.6% in average.

Although our method is trained and tested on each test image, it has almost the same execution time compared with CCADN, due to the significantly reduced network complexity and faster convergence brought by the internal visual entropy.

3.2 Medical Image Segmentation

CHD usually comes with significant variations in heart structures and great vessel connections, which renders general whole heart and great vessel segmentation methods [8] [9] in normal anatomy ineffective. Most existing segmentation methods dedicated to CHD target blood pool and myocardium only [10] [11]. Recently, semi-automated segmentation in CHD has also been explored [12], which requires users to locate an initial seed. However, fully automated segmentation of whole heart and great vessel segmentation in CHD still remains a missing piece in the literature. Inspired by the success of graph matching in a number of applications with large variations [13], we propose to combine deep learning [14] and graph matching for fully automated whole heart and great vessel segmentation in CHD. Particularly, we leverage deep learning to segment the four chambers and myocardium followed by blood pool, where variations are usually small and accuracy can be high. We then extract the vessel connection information and apply graph matching to determine the categories of all the vessels.

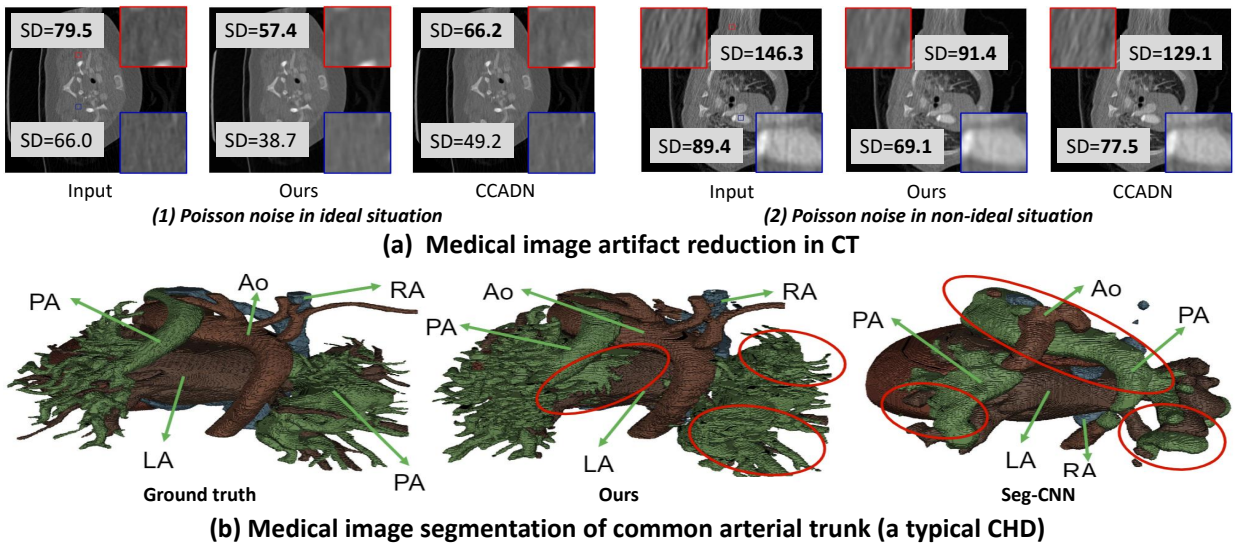

Figure 3: Performance of AI-CHD in each step.

The overall flow for whole heart and great vessel segmentation (left ventricle (LV), right ventricle (RV), left atrium (LA), right atrium (RA), myocardium (Myo), aorta (Ao), and pulmonary artery (PA)) contains two modules: whole heart segmentation, and great vessel segmentation. In whole heart segmentation, RoI cropping is firstly presented to extract the area that includes the heart and its surrounding vessels. We resize the input image to a low resolution of 64×64×64, and then adopt the same segmentation-based extraction as [9] to get the RoI. The RoI is then resized to 64×64×64 which is fed to a 3D U-net [15] for segmentation. In great vessel segmentation, blood pool segmentation is conducted on each 2D slice of the input using a 2D U-net [16] with an input size of 512×512. Note that in order to detect the blood pool boundary for easy graph extraction in graph matching later, we add another class blood pool boundary in the segmentation. With the high-resolution blood segmentation, whole heart segmentation achieves chambers and myocardium refinement by refining the boundaries of chambers and myocardium. By removing the blood pool corresponding to the low-resolution whole heart segmentation, great vessel segmentation obtains the blood pool corresponding to the great vessels, and adopts graph matching to identify Ao, PA and anomalous vessels.

For evaluation we collected a dataset composed of 68 3D CT images captured by a Simens biograph 64 machine. The ages of the associated patients range from 1 month to 21 years, with majority between 1 month and 2 years. The size of the images is $512 \times 512 \times (130-340)$, and the typical voxel size is $0.25 \times 0.25 \times 0.5 mm^3$. The dataset covers 14 types of CHD, which include six common types (atrial septal defect (ASD), atrio-ventricular septal defect (AVSD), patent ductus arteriosus (PDA), pulmonary stenosis (PS), ventricular septal defect (VSD), co-arctation (CA)) plus eight less common ones (Tetrology of Fallot (ToF), transposition of great arteries (TGA), pulmonary artery sling (PAS), anomalous drainage (AD), common arterial trunk (CAT), aortic arch anomalies (AAA), single ventricle (SV), pulmonary atresia (PuA)). All labeling were performed by experienced radiologists, and the time for labeling each image is 2-3 hours. The labels include seven substructures: LV, RV, LA, RA, Myo, Ao and PA. For easy processing, venae cavae (VC) and pulmonary vein (PV) are also labeled as part of RA and LA respectively, as they are connected and their boundaries are relatively hard to define. Anomalous vessels are also labeled as one of the above seven substructures based on their connections.

The comparison with Seg-CNN [9] is shown in Table 1. Our method can get 5.8%-19.2% higher

Table 1: Mean and standard deviation (SD) of Dice score of the state-of-the-art method Seg-CNN [9] and our method (in %) for seven substructures of whole heart and great vessel segmentation.

Method		LV	RV	LA	RA	Myo	Ao	PA	Average
Seg-CNN [9]	Mean	67.3	65.0	70.2	76.0	71.5	63.0	52.3	66.5
	SD	±13.9	±12.0	±7.8	±7.5	±8.3	±13.3	±12.3	±10.7
Our method	Mean	82.4	77.6	78.6	82.7	77.3	82.2	67.1	78.3
	SD	±10.5	±14.3	±7.4	±7.5	±8.3	±8.1	±19.8	±10.8

mean Dice score across the seven substructures (12% higher on average) with almost the same standard deviation. The highest improvement is achieved in Ao, which is due to its simple graph connection with successful graph matching. The least improvement is obtained in myocardium, which is due to the fact that myocardium is not well considered in the high-resolution blood pool segmentation. Visualization of CAT segmentation using our method and Seg-CNN is shown in Figure 3(b). Our method can clearly segment Ao and PA with some slight mis-segmentation between PA and LA. However, Seg-CNN segments the main part of Ao as PA, which is due to the fact that pixel-level segmentation by U-net is only based on the surrounding pixels, and the connection information is not well exploited.

3.3 Real-time Video and Audio Transmission

Real-time video and audio transmission is also a critical part in surgical telementoring. Such transmission needs to have high data rate and low latency so that important decisions can be made in real time to avoid potential complications. In addition, in an operating room, wireless transmission is always preferred over wired transmission. The most common wireless transmission method so far, 4th generation wireless communication (4G) is with about 50ms latency and a data rate of 10 million bits per second (10 Mbps) in average. With such moderate transmission quality, some less complex procedures such as addiction management [17] and training [18] can be performed using telementoring.

Currently 5th generation wireless communication is emerging with about 10ms latency (1ms in special cases) and a high data rate of 50+ Mbps on average. Such high transmission quality has enabled a lot of complex procedures, including intestinal tumor procedure [19], liver removal of a laboratory test animal [20], laparoscopic cholecystectomy [21], and gall bladder surgery [22]. However, so far there is no surgical telementoring of cardiac surgery for CHD treatment reported, possibly due to the extremely high complexity and high risk involved.

4 Case Study

On April 3rd 2019, we used AI-CHD to perform the first 5G based heart telementoring in China with collaboration between Guangdong Provincial Peoples Hospital (GPPH) and the People's Hospital of Gaozhou (PHG). The 5G communication is provided by Guangdong Mobile Communications Group and Huawei. In the telementoring, AI-CHD produced accurate heart model of the patient, which was then used for surgical planning and training before the surgery and real-time guidance during the surgery.

The 41-year-old patient Ms Green (alias) from Gaozhou, Guangdong Province complained about her shortness of breath, chest pain, difficulty in walking and insomnia. She was then diagnosed with atrial septal defect (ASD) with tricuspid insufficiency, severe pulmonary hypertension,

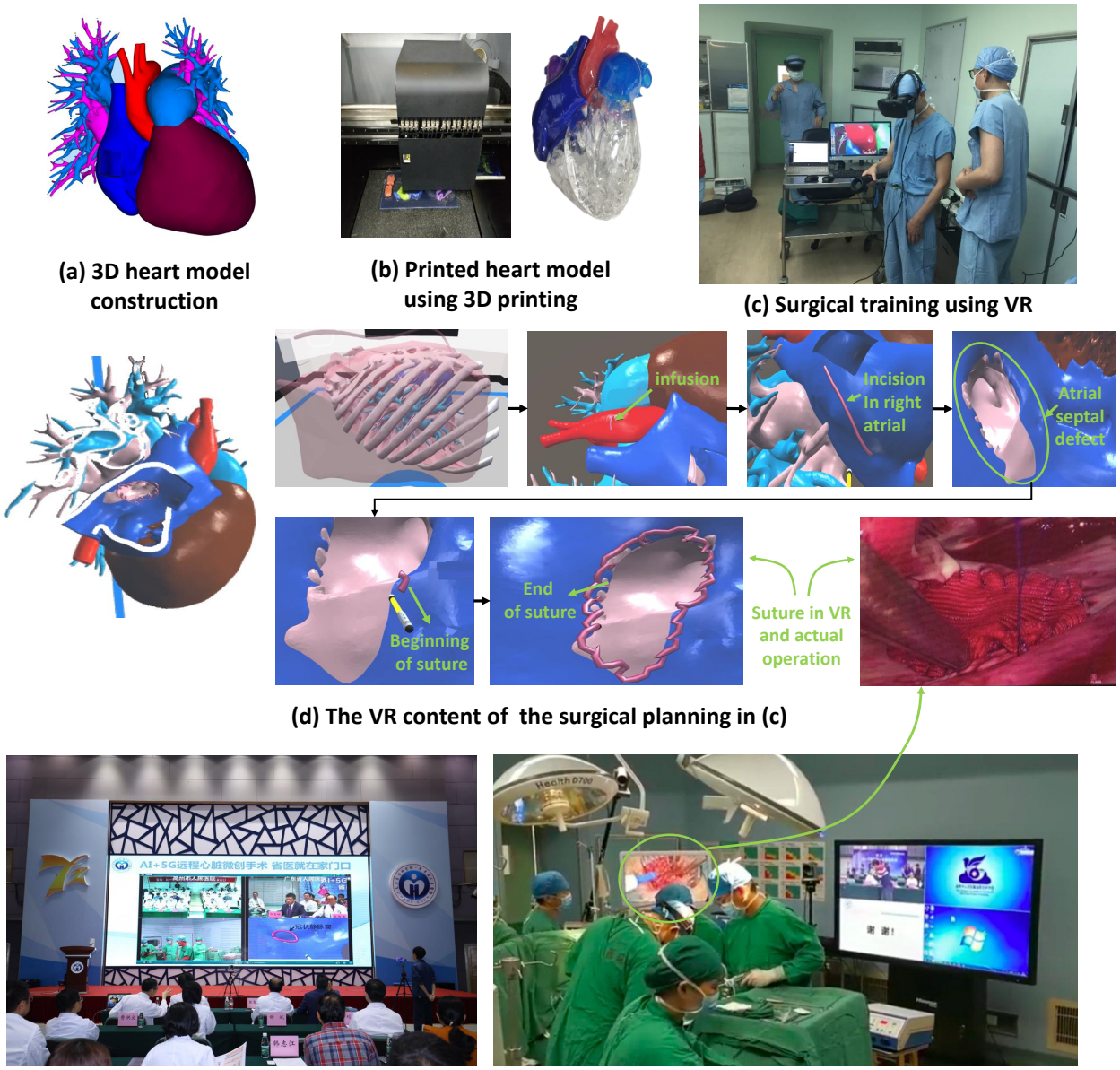

Figure 4: Case study of AI-CHD: telementoring for a patient with atrial septal defect is performed between Guangdong Provincial Peoples Hospital (GPPH) and the People's Hospital of Gaozhou (PHG) in April 3rd, 2019. These two hospitals are 250 miles away from each other. The 3D heart model in (a) obtained from AI-CHD is used for (b) heart model printing and (c) surgical training. In (c) surgical training, surgeons can practice the surgery in VR which is also based on the 3D heart model in (a). The telementoring is successfully performed, and some on-site photos of the event are shown in (e).

and cardiac failure at PHG. In fact, ASD is a moderate type of CHD. If well treated at a young age, the operation is relatively easy and the risk is low. However, due to the lack of screening in rural areas, the patient was already at her middle age, missing the best time for treatment. In addition, due to the long-time disordered operation of the heart, she also suffered from severe pulmonary hypertension and began to have heart failure. Thus, the condition had changed from a relatively

simple CHD to a complex one, and only surgery could "save the heart".

Being in a less developed region, surgeons at PHG only have experience in conventional open-heart surgery which is with high risk, especially for a long suffering patient with weak physique like Ms Green. Minimally invasive surgery is preferred for Ms Green which is with much less risk, but much higher complexity. However, the nearest hospital with expert surgeons for such a surgery is GPPH, one of the largest cardiac medical centers in China which is about 250 miles away from PHG. Considering the weak physique of Ms Green, long-distance transportation is not feasible. Therefore, telementoring is the most suitable approach for Ms Green. With comprehensive discussion and analysis, Dr. Huiming Guo, the chief physician of cardiac surgery department of GPPH, agreed to be the telementor in this telementoring surgery. Dr. Guo is good at minimally invasive surgery and enjoys an international reputation in the surgical treatment of CHD.

Before Ms Green's surgery, we first collected her 3D cardiac CT images from PHG. AI-CHD then produced her 3D heart model as shown in Figure 4(a), with clinically acceptable accuracy of 0.81 Dice score for the surgery. The runtime was less than 2 minutes, much faster than the manual segmentation which would otherwise take 2-3 hours or even longer, thus significantly reducing the cost. With the 3D heart model surgical planning and training were then performed. As shown in Figure 4(b), the heart model was first printed out with a 3D printer (thin vessels of pulmonary artery and pulmonary vein were removed as they were not related to the surgery). The printed model gave a straightforward view of the heart's appearance and structure and where the problem was. Dr. Guo discussed the surgical plan with other members of his team as well as the remote team at PHG using the printed model. Once the plan was laid, virtual surgical training was then carried out with virtual reality (VR) technology as shown in Figure 4(c). As shown in Figure 4(d), VR enables the doctors to enlarge and shrink specific structures of the heart including its inner structures, and perform virtual operations such as infusion and suture as a practice. In this way, Dr. Guo could get a comprehensive understanding of the surgery to be telemonitored and know the best operations/parameters for effective guidance.

After Dr. Guo confirmed the surgical planning and the detailed process with the help of AI-CHD, telementoring of Ms Green's surgery started at 9:35 AM, April 3rd, 2019. The pictures of the guidance at GPPH and the actual surgery operation at PHG are shown in Figure 4(d). In the telemenrtoring, there were totally four real-time video streams: the view of the surgeon, and the corresponding VR view of the heart, the scene of the telementor (Dr. Huiming Guo), and the scene of the operation room. Note that as this was the first telementoring of CHD surgery in China, doctors from cardiac surgery, cardiac ultrasound and cardiac imaging departments all participated to observe this event as shown in the view of the telementor. Based on the real-time view of the surgeon and the corresponding VR scene, Dr. Guo could easily recognize the current viewpoint in the heart and give immediate guidance via a real-time audio stream. For example, when determining the opening point at the pericardium, the the surgeon asked "should the pericardium be opened here?" Dr. Guo answered immediately: "move up 3 centimeters." For the suture in the operation which is also the key part in the invasive heart surgery, Dr. Guo also reminded that "Do not be too close to the Koch's triangle when stitching; otherwise it is easy to cause myocardial injury and block the heart beating rhythm conduction". The Koch's triangle was drawn in VR video and shown to the surgeons at the operation room 250 miles away in real-time.

Throughout the telemonitoring, the transmission rate for video streams is stabilized at around 25 Mbps with a latency of 30 ms. The surgery was carried out smoothly and finished at 1:00 PM. The heart was sutured and Ms. Green's heart resumed beating. After a week's recovery, she was discharged from hospital. The postoperative review showed that the pulmonary artery pressure and mitral regurgitation were within the normal range. As of the day this article was written (December 1, 2019). the patient remains in a good condition. Our case study has received

extensive media coverage including the biggest and most influential news organizations in China Xinhua [23] and Global Times [24].

5 Looking Forward

This is the third year of collaboration between computer scientists, cardiac surgeons, and radiologists in our team. The original works of artifact reduction and segmentation of cardiac CT images have gradually evolved into a holistic system of 3D heart model construction. In the future, in addition to the further optimization of AI-CHD, we plan to explore the following two promising areas for automatic and cost-efficient treatment of CHD:

Automatic diagnosis: Accurate diagnosis of CHD is more significant compared with artifact reduction and segmentation. Due to the lack of CHD diagnosis experience in developing regions, many cases are not diagnosed correctly and missed timely treatment [1]. On the other hand, an experienced radiologist needs proper training for more than 10 years which is slow and costly. In addition, even an experienced radiologists may need up to half an hour to diagnose a patient with CHD. Thus, automatic diagnosis of CHD is preferred, which can provide high-quality and cost-efficient medical care in a large scale. To be clinically acceptable, such automatic CHD diagnosis need also report the features or reasons for the diagnosis with a confidence score. The feature or reasons can let the radiologists easily verify the results, while low confidence scores can suggest cases that need manual diagnosis.

Automatic surgery planning: Due to the large structure variations in CHD, there exists tens of surgical procedures, each containing parameters such as the opening point, and the size and direction of an incision. Currently surgeons make surgical plannings based on their experience which may or may not be the optimal choice in terms of prognosis. We will further extend AI-CHD to enable accurate automatic surgical planning for optimal treatment.

6 Conclusion

AI-CHD is an accurate AI-based framework for surgical telementoring of CHD. It is developed through deep collaborations between computer scientists, radiologists and surgeons. The technology enables cost-effective and timely model construction of hearts in CHD, which assists radiologists and surgeons to perform efficient surgical planning and training in CHD surgery, as demonstrated by the case study reported. AI-CHD can reduce the cost while improve the quality of telementoring of CHD surgery in developing countries and regions.

7 Acknowledgement

This work was approved by the Research Ethics Committee of Guangdong General Hospital, Guangdong Academy of Medical Science under Protocol No. 20140316. This work was approved by the Research Ethics Committee of Guangdong General Hospital, Guangdong Academy of Medical Science under Protocol No. 20140316. This work was supported by the National key Research and Development Program of China (2018YFC1002600), the Science and Technology Planning Project of Guangdong Province, China (No.2017B090904034, 2017B030314109, 2018B090944002, 2019B020230003), Guangdong Peak Project (DFJH201802), and the National Natural Science Foundation of China (No.62006050).

References

[1] D. Ntiloudi, G. Giannakoulas, D. Parcharidou, T. Panagiotidis, M. A. Gatzoulis, and H. Karvounis, "Adult congenital heart disease: a paradigm of epidemiological change," *International journal of cardiology*, vol. 218, pp. 269–274, 2016.

[2] L. W. Nifong, V. F. Chu, B. M. Bailey, D. M. Maziarz, V. L. Sorrell, D. Holbert, and W. R. Chitwood Jr, "Robotic mitral valve repair: experience with the da vinci system," *The Annals of thoracic surgery*, vol. 75, no. 2, pp. 438–443, 2003.

[3] J. Marescaux and F. Rubino, "The zeus robotic system: experimental and clinical applications," *Surgical Clinics*, vol. 83, no. 6, pp. 1305–1315, 2003.

[4] M. Zontak and M. Irani, "Internal statistics of a single natural image," in *Computer Vision and Pattern Recognition (CVPR), 2011 IEEE Conference on*. IEEE, 2011, pp. 977–984.

[5] J. M. Wolterink, T. Leiner, M. A. Viergever, and I. Išgum, "Generative adversarial networks for noise reduction in low-dose ct," *IEEE transactions on medical imaging*, vol. 36, no. 12, pp. 2536–2545, 2017.

[6] Q. Yang, P. Yan, Y. Zhang, H. Yu, Y. Shi, X. Mou, M. K. Kalra, Y. Zhang, L. Sun, and G. Wang, "Low dose ct image denoising using a generative adversarial network with wasserstein distance and perceptual loss," *IEEE transactions on medical imaging*, 2018.

[7] E. Kang, H. J. Koo, D. H. Yang, J. B. Seo, and J. C. Ye, "Cycle consistent adversarial denoising network for multiphase coronary ct angiography," *arXiv preprint arXiv:1806.09748*, 2018.

[8] C. Wang, T. MacGillivray, G. Macnaught, G. Yang, and D. Newby, "A two-stage 3d unet framework for multi-class segmentation on full resolution image," *arXiv preprint arXiv:1804.04341*, 2018.

[9] C. Payer, D. Štern, H. Bischof, and M. Urschler, "Multi-label whole heart segmentation using cnns and anatomical label configurations," in *International Workshop on Statistical Atlases and Computational Models of the Heart*. Springer, 2017, pp. 190–198.

[10] L. Yu, X. Yang, J. Qin, and P.-A. Heng, "3d fractalnet: dense volumetric segmentation for cardiovascular mri volumes," in *Reconstruction, segmentation, and analysis of medical images*. Springer, 2016, pp. 103–110.

[11] J. M. Wolterink, T. Leiner, M. A. Viergever, and I. Išgum, "Dilated convolutional neural networks for cardiovascular mr segmentation in congenital heart disease," in *Reconstruction, segmentation, and analysis of medical images*. Springer, 2016, pp. 95–102.

[12] D. F. Pace, A. V. Dalca, T. Brosch, T. Geva, A. J. Powell, J. Weese, M. H. Moghari, and P. Golland, "Iterative segmentation from limited training data: Applications to congenital heart disease," in *Deep Learning in Medical Image Analysis and Multimodal Learning for Clinical Decision Support*. Springer, 2018, pp. 334–342.

[13] S. M. Lajevardi, A. Arakala, S. A. Davis, and K. J. Horadam, "Retina verification system based on biometric graph matching," *IEEE transactions on image processing*, vol. 22, no. 9, pp. 3625–3635, 2013.

[14] X. Xu, Q. Lu, L. Yang, S. Hu, D. Chen, Y. Hu, and Y. Shi, "Quantization of fully convolutional networks for accurate biomedical image segmentation," in *Proceedings of the IEEE Conference on Computer Vision and Pattern Recognition*, 2018, pp. 8300–8308.

[15] Ö. Çiçek, A. Abdulkadir, S. S. Lienkamp, T. Brox, and O. Ronneberger, "3d u-net: learning dense volumetric segmentation from sparse annotation," in *International conference on medical image computing and computer-assisted intervention*. Springer, 2016, pp. 424–432.

[16] O. Ronneberger, P. Fischer, and T. Brox, "U-net: Convolutional networks for biomedical image segmentation," in *International Conference on Medical image computing and computer-assisted intervention*. Springer, 2015, pp. 234–241.

[17] M. R. Sagi, G. Aurobind, P. Chand, A. Ashfak, C. Karthick, N. Kubenthiran, P. Murthy, M. Komaromy, and S. Arora, "Innovative telementoring for addiction management for remote primary care physicians: A feasibility study," *Indian journal of psychiatry*, vol. 60, no. 4, p. 461, 2018.

[18] E. M. Bogen, K. M. Augestad, H. R. Patel, and R.-O. Lindsetmo, "Telementoring in education of laparoscopic surgeons: An emerging technology," *World journal of gastrointestinal endoscopy*, vol. 6, no. 5, p. 148, 2014.

[19] W. R. Academy, "Worlds first 5g-powered surgery: Dr. antonio de lacy," 2019, https://www.worldrecordacademy.org/medical/worlds-first-5g-powered-surgery-dr-antonio-de-lacy-219142.

[20] A. Cuthbertson, "Surgeon performs world's first remote operation using '5g surgery' on animal in china," 2019, https://www.independent.co.uk/life-style/gadgets-and-tech/news/5g-surgery-china-robotic-operation-a8732861.html.

[21] Xinhua, "5g remote surgery conducted in central china," 2019, http://www.xinhuanet.com/english/2019-06/11/c_138134223.htm.

[22] PTI, "Chinese surgeons conduct remote surgery using 5g technology," 2019, https://timesofindia.indiatimes.com/world/china/chinese-surgeons-conduct-remote-surgery-using-5g-technology/articleshow/69742530.cms.

[23] Xinhua, "5g remote guided cardiac minimally invasive surgery completed in guangdong," 2019, http://xhpfmapi.zhongguowangshi.com/vh512/share/5926348.

[24] G. Times, "First ai+5g surgery completed with huaweis technological support," 2019, http://www.globaltimes.cn/content/1144600.shtml.